Ionic Liquid-Based Safe Adjuvants

Anvay Ukidve, Katharina Cu , Morgan Goetz, Pavimol Angsantikul, Alexander Curreri, Eden E.L. Tanner, Joerg Lahann, Samir Mitragotri*

A. Ukidve, K. Cu, M. Goetz, Dr. P. Angsantikul, A. Curreri, Dr. E.E.L. Tanner, Prof. S. Mitragotri

John A. Paulson School of Engineering and Applied Sciences

Harvard University

Cambridge, MA 02138, USA

Email: mitragotri@seas.harvard.edu

A. Ukidve, M. Goetz, Dr. P. Angsantikul, A. Curreri, Dr. E.E.L. Tanner, Prof. S. Mitragotri

Wyss Institute of Biologically Inspired Engineering

Harvard University

Boston, MA 02115, USA

Prof. J. Lahann

Department of Chemical Engineering, Materials Science and Engineering, Biomedical Engineering, and Macromolecular Science and Engineering

University of Michigan

Ann Arbor, MI 48105, USA

A.U. and K.C. contributed equally.

Abstract:

Adjuvants play a critical role in the design and development of novel vaccines. Despite extensive research, only a handful of vaccine adjuvants have been approved for human use. Currently used adjuvants mostly comprise of components which are non-native to the human body, such as aluminum salt, bacterial lipids or foreign genomic material. Here, a new ionic liquid-based adjuvant is explored, synthesized using two metabolites of the body, choline and lactic acid (ChoLa). ChoLa distributes the antigen efficiently upon injection, maintains antigen integrity, enhances immune infiltration at the injection site, and leads to a potent immune response against the antigen. Thus, it can serve as a promising safe adjuvant platform that can help to protect against pandemics and future infectious threats.

The current COVID-19 pandemic has brought vaccines to the forefront of medical, societal and economic challenges. Adjuvants form an important, and often essential, component of effective vaccines.[1] According to the Centers of Disease Control and Prevention (CDC), several materials have been explored for use as adjuvants, although only a few including aluminum salts (alum), bacterial lipids (monophosphoryl A) and foreign genome (CpG) are commonly used. A key reason for this limited translation of adjuvants is the safety concern.[2] While a large effort is currently being focused on developing novel vaccines for COVID-19 (115 candidates as of April 8, 2020), an alarmingly small effort is focused on developing novel adjuvants.[3] Any effort to design better vaccines against COVID-19 and future infectious threats must include a strong effort to expand the

current toolbox of adjuvants. Design of potent and safe adjuvants poses a significant challenge since they must strike a delicate balance between strong local immune stimulation and low systemic toxicity.[4] We sought to address this challenge using biocompatible ionic liquids.

Ionic liquids and deep eutectic solvents represent a class of synthetic materials with a high degree of tunability and manufacturability.[5] They can be synthesized from components that are "generally regarded as safe" (GRAS),[6] thus improving their safety profile. ILs have been developed and used for drug delivery applications; however, their use as an adjuvant has not been yet explored. Here we report a novel liquid adjuvant, Choline and Lactic acid (ChoLa), and using ovalbumin as a model antigen, we show that ChoLa improved antigen dispersion, induced potent antigen-presenting cell (APC) infiltration at the site of injection, and generated a strong immune response against the antigen (**Figure S1, Supporting Information**).

Choline and Lactic acid are natural and abundantly occurring metabolites in the human body. Further, they both have status as Generally Recognized as Safe (GRAS) molecules. ChoLa (Cho:La molar of 1:2) was synthesized using salt metathesis and was verified by ^{1}H- NMR spectroscopy (**Figure S2, Supporting Information)**. Neat ChoLa is a colorless viscous liquid which forms a milky emulsion upon dilution in saline, likely due to formation of micron-sized globules (Figure S3, Supporting Information). OVA was chosen for our studies due to extensive characterization of its immunological and structural attributes. Upon addition to ChoLa (10% w/v in saline), OVA associated with the ChoLa emulsion (**Figure 1a, Figure S4, Supporting Information**) and was released over 24 h. (**Figure 1b**). Compared to alum, ChoLa exhibited lower adsorption and faster release of the adsorbed OVA (**Figure 1a, b**). The injection of OVA-alum and OVA-ChoLa in *ex vivo* porcine skin showed that adjuvants significantly impact antigen spreading. ChoLa induced a significantly greater spread of the antigen in the skin compared to alum (**Figure 1c, d, Figure S5,**

Supporting Information). Increasing the concentration of ChoLa decreased the spread, likely due to higher viscosity (**Figure S6a-b, Supporting Information**). At the same time, increase in ChoLa concentration decreases the stability of OVA, hence reduced epitope stability is obtained with an increase in ionic liquid concentration (**Figure S7, Supporting Information**). Thus, 10 % ChoLa was investigated for its adjuvant properties in the current study. SDS-PAGE indicated that ChoLa maintained the molecular integrity of adsorbed OVA similar to alum and saline (**Figure 1e**). Circular Dichroism analysis showed that the secondary structure of OVA, composed majorly of α- helices, is preserved by 10% ChoLa (**Figure 1f)**

The effect of ChoLa and alum on the local immune environment was assessed by subcutaneously injecting into mice and measuring the draining lymphocytes after 24h. ChoLa-treated mice showed a 20% higher infiltration of dendritic cells compared to untreated and alum-treated mice (**Figure 2a, Figure S8, Supporting Information**). More importantly, these dendritic cells also showed a significant increase in CD 86, a marker for activation, compared to the controls (**Figure 2b**). Along with dendritic cells, a ~25% increase in infiltration of CD4+ cells was observed for the ChoLa group, compared to the controls (**Figure 2c**), indicating further antigen presentation/cross-presentation,[7] demonstrating the potential to induce a strong systemic immune response. Infiltrating CD8+ cells showed no such effect (**Figure S9, Supporting Information**).

Finally, we evaluated the ability of ChoLa to induce immune responses. Mice were immunized by once a week injection for a total of three weeks (**Figure S10a, Supporting Information**). In parallel, systemic toxicity of treatments was assessed by monitoring the body weight (**Figure S10b, Supporting Information**). Two-way ANOVA analysis indicated that the treatment groups minimally affected the change in body weight. Both *Th1* and *Th2* responses to OVA were assessed. ChoLa induced a non-significant *Th2* response, as assessed by anti-OVA IgG,

compared to alum (**Figure 3a)**. On the contrary, a strong *Th1* response was observed in the ChoLa group. ChoLa led to a 5-fold increase in the CD8+ cells compared to the controls (**Figure 3b**). This was accompanied by a ~ 1.8-fold increase in natural killer (NK) cells compared to the saline group (**Figure 3c**). ChoLa group also had significantly higher activated dendritic cells (CD80) (**Figure 3d**). ChoLa increased the number of CD4+ cells by 50% compared to both the other groups. On characterizing the CD4 population further, a ~3-fold increase in IFN- γ+ CD4+ cells was observed for ChoLa compared to alum (**Figure 3e**). All these are markers of a potent *Th1* type cellular immune response.[8] *Th1* response plays a crucial role in the fight against viral infections.

Literature suggests that novel adjuvants, in their early developmental stage, be compared and benchmarked against the more established adjuvant Alum as a gold standard[9]. Hence, in our studies, we compared ChoLa to Alum. In future studies, this adjuvant platform should be compared with other emulsion-based adjuvants such as MF59 or AS03. The results presented here demonstrate the ability of ChoLa to induce a strong *Th1* immune response. ChoLa globules achieve active immune infiltration at the site of injection likely due to its physical form as well as the constituent lactic acid which itself is immunostimulatory. Due to this mechanism of adjuvancy as well as the physical form of ChoLa, adsorption of protein on the globules will help in their efficient uptake and priming by the infiltrated immune cells. Multiple antigen loading can be optimized by tweaking surface properties of the globules by the inclusion of surfactant systems. Future studies should investigate this possibility. Even at this early development stage, ChoLa has clear benefits with regards to manufacturability, reduced material variability, mechanism of adjuvancy as well as safety.

The mechanism of action of ChoLa is attributed to immune modulation at the site of action and can be positively altered by increasing its concentration. However, we expect it to be a

balancing act of two completely different phenomena- the effect of the ChoLa concentration on the antigen stability and the potential toxicity at the site of injection associated with higher concentrations of ChoLa. For effective adjuvant properties, we need to ensure that the antigen epitope is stable as well as ensure the immune modulation at the site of action without systemic inflammation. We did investigate the effect of concentration of ChoLa on protein stability and observed that an increase in ChoLa concentration leads to changes in CD spectra indicating potential loss of secondary structure. Potential toxicity arising from high ChoLa concentration should be explored in detail with future studies. A complete understanding of these effects is necessary to determine optimal concentrations of ChoLa.

To our knowledge, this is the first report on the use of ionic liquids as adjuvants. We demonstrated the stability of a clinically relevant antigen, SARS-Cov-2 spike protein (**Figure S11, Supporting Information**), in ChoLa. Lastly, we also explored the ability of ChoLa to be used with other adjuvants like Alum and CpG. ChoLa adsorbs onto the surface of Alum without compromising formulation stability (**Figure S12a-b, Supporting Information**). ChoLa can also admix with CpG while maintaining its structural integrity (**Figure S12c, Supporting Information**). This emphasizes the versatility of the ionic liquid adjuvant platform, which could be used with other available adjuvants for generating broad-spectrum immunity. All in all, this study demonstrates the feasibility of using ChoLa as an adjuvant.

With additional research on safety and efficacy against specific viral threats, ChoLa and ionic liquids in general, could offer a notable addition to the repertoire of available adjuvants for addressing unmet needs for protection against pandemics like COVID-19 and future infectious agent threats.

Experimental Section

Materials: All chemicals and reagents were obtained from Sigma Aldrich and used without further purification unless otherwise mentioned. Amicon Ultra-0.5 centrifugal filters were also obtained from Sigma Aldrich. FITC-OVA was purchased from Thermo Fisher. Alhydrogel and OVA-Alexa Fluor 647 were purchased from Invitrogen. EndoFit® Ovalbumin was purchased from Invivogen. 0.9 % saline solution was obtained from Teknova. Sodium phosphate buffer was purchased from Boston BioProducts. Tissue Tek OCT compound was obtained from Sakura Finetek. CpG was purchased from IDT technologies. SARS-Cov-2 Spike protein was purchased from ABClonal Technology. Positively charged glass slides were purchased from Fisher Scientific. Rectangular quartz cells with a 1 mm path length (1-Q-1) were obtained from Starna Cells. Laemmli protein sample buffer, 4–15% 12-well precast polyacrylamide gel, Tris/glycine/SDS running buffer, Mini-PROTEAN Tetra Cell Electrophoresis System, Precision Plus Protein™ All Blue Prestained Protein Standards and Bio-Safe Coomassie Stain were purchased from BioRad Laboratories. Porcine skin was obtained from Lampire Biological Laboratories. Surgical equipment was obtained from Braintree Scientific, Inc.

Synthesis and characterization of choline lactate (1:2) (ChoLa): Choline bicarbonate (80% in water) was combined, with vigorous stirring, with lactic acid (85%) in a 1:2 molar ratio at 40 °C. The mixture was left stirring overnight, then placed under rotary evaporation at 10 mbar and 60 °C for 2 h, before being put in a vacuum oven at 60 °C for 72 h. The resulting product was a light-yellow viscous liquid, whose chemical identity was confirmed by Nuclear Magnetic Resonance Spectroscopy. ^{1}H NMR (600 MHz, d-DMSO) 1.2 (m, 6H, C$\underline{H}_3$CH(OH)COO; C$\underline{H}_3$CH(OH)COOH); 3.09 (s, 9H, NC$\underline{H}_3$); 3.38 (h, 2H, NC$\underline{H}_2$CH$_2$OH); 3.80 (m, 4H, CH$_3$C$\underline{H}$(OH)COO; CH$_3$C$\underline{H}$(OH)COOH; NCH$_2$C$\underline{H}_2$OH).

Formulation Preparation: 0.5 mg mL^{-1} ovalbumin, Alexa Fluor 647/FITC-labeled ovalbumin for in vitro experiments were dissolved in saline. For the ChoLa adjuvant formulation, 10% w/v ChoLa was added unless specified.

Globule/ Particle size distribution: Globule size distribution for 10% ChoLa in saline was evaluated using dynamic light scattering (Zetasizer, Malvern). Particle size distribution and zeta potential for alum microparticles with/ without 10% ChoLa were also determined similarly.

In vitro drug release study: OVA containing solutions (0.5 mg mL^{-1}) and complete medium (DMEM + 10% FBS) were mixed to a total volume of 500 µL and incubated at 37°C on a tube revolver. At regular time points, the suspensions were centrifuged at 12 000 x g for 15 min and the supernatant was collected for analysis. The pellet was further resuspended in 400 µL fresh release media and incubated until the next time point. Samples were taken at 1, 2, 4, 6, 12, 24, 48 and 72 h after starting the incubation. OVA was separated from residual ionic liquid using a centrifugal filter. The cumulative release in each release medium was quantified using OVA as fluorophore (Ex/Em 633/665) on a plate reader (Spectramax i3).

In vitro dispersion: 50 µL of OVA-saline (0.5 mg mL^{-1}), OVA-ChoLa (0.5 mg mL^{-1}) or alum (2% suspension) were subcutaneously injected into *ex vivo* porcine skin. The samples were incubated for 5 h at 37 °C before frozen in optimum cutting temperature compound and sectioned into 15 µm thin slices using a cryostat (CM1950 Leica Biosystems). The tissue sections were collected on positively charged glass slides and imaged on a fluorescent microscope (Axio Zoom V16, Zeiss). The horizontal

and vertical solution diffusion throughout the skin samples (width and depth) were analyzed with the image processing software ImageJ. Further, a MATLAB code developed for image processing was used to determine the surface area of the injection site.[10]

Assessment of protein/CpG stability: SDS-PAGE assay and circular dichroism were carried out to assess protein aggregation and conformation from the ChoLa or alum samples. 1 mg mL^{-1} OVA in 10-40 % v/v ChoLa or 2% alum were incubated for 1 h at room temperature (25 °C). protein in saline was used as a negative control. The samples were then dialyzed in 10 mM pH 7.4 sodium phosphate buffer (Boston BioProducts) for 48 h. Before electrophoresis, all samples were adjusted to equivalent protein concentration. The samples were then mixed with Laemmli protein sample buffer and separated on a 4–15% 12-well precast polyacrylamide gel in Tris/glycine/SDS running buffer using a Mini-PROTEAN Tetra Cell Electrophoresis System (BioRad). The protein bands were stained with Bio-Safe Coomassie stain (BioRad) for observation according to the manufacturer's protocol. In parallel, the three OVA samples were analyzed by circular dichroism spectrophotometry (Jasco J-1500, Easton) in the far-UV region (190-250 nm). Rectangular quartz cells with a 1 mm path length (1-Q-1) were loaded with 400 µL of a sample. As a control spectrum, OVA in PBS was used. Each spectrum was the average of five scans. Similar process was carried out for SARS-Cov-2 Spike protein (0.1 mg mL^{-1}) and CpG (0.25 mg mL^{-1})

Animals: Female Balb/C mice (6-8-week-old) were purchased from Charles River Laboratories.

In vivo injection site modulation studies: Balb/c mice were subcutaneously injected in the back with 50 µL of saline, ChoLa or alum (n=4 for all groups). 24 h after injections, the skin from the injection site was harvested, cut into 0.5 – 2 mm^2 pieces and incubated with collagenase D (2 mg mL^{-1}), DNAse I (0.2 mg mL^{-1}), RPMI-1640 in a total volume of 5 mL PBS for 45 min at 37°C on a tube revolver. Undigested tissue was removed by 70 µm mesh filtration. The suspension was centrifuged at 400 x g for 10 min. The supernatant was removed via pipetting and 2 mL ACK lysing buffer (Thermo Fisher) was added to the pellet. After 5 min the suspensions were centrifuged again and resuspended with 2 mL FCS blocking buffer.

In vivo vaccination studies: Balb/c mice were subcutaneously injected in the back with 50 µL of OVA-saline, OVA-ChoLa or alum (n=8 for all groups). A total of three injections were given on day 0, day 7 and day 14. On day 19, the mice were euthanized, blood and spleen were collected for further analysis.

Antibody titer measurements: Blood was centrifuged at 5000 rpm for 10 minutes at 4°C to separate the serum from the cells. Anti- OVA IgG titer was measured as previously described.[11]

Immune cell profiling: Antibody cocktails were made from CD45 (Biolegend, Cat no: 103116, Clone: 30-F11), CD 3 (Biolegend, Cat no: 100218, Clone: 17A2), CD4 (Biolegend, Cat no: 100421, Clone: GK1.5), CD8a (Biolegend, Cat no: 100711, Clone: 53-6.7), NKp46 (Biolegend, Cat no: 137606, Clone: 29A1.4), CD 11c (Biolegend, Cat no: 117307, Clone: N418), IFN- γ (Biolegend, Cat no: 505849, Clone:

XMG1.2, CD86 (Biolegend, Cat no: 105011, Clone: GL-1), and Am Cyan Live/dead cell staining kit (Thermo Fischer Scientific, MA, USA). All antibodies were diluted at least 200 times prior to their use.

Statistical analyses: Statistical significance was analyzed using a two-tailed t-test, one- or two-way analysis of variance with Tukey's multiple-comparison test. p values represent different levels of significance; $p < 0.05$ *; $p < 0.01$ **; $p < 0.001$ ***. Fluorescent images were analyzed using ImageJ. Flow cytometry graphs were analyzed using FCS Express 7.0. All data analysis was carried out with Graphpad Prism v8.0.

Supporting Information

Supporting Information is available from the Wiley Online Library or from the author.

Ethical Statement

All experiments were performed according to the approved protocols by the Institutional Animal

Care and Use Committee (IACUC) of the Faculty of Arts and Sciences (FAS), Harvard University,

Cambridge.

Conflict of interest

SM, AU and KC are inventors on patent applications related to the technology described in the

manuscript. PA, EELT and SM are inventors on patent applications related to ionic liquids. SM is a

board member/shareholder/consultant of Liquideon LLC, CAGE Bio and i2O Therapeutics.

References

[1]   A. Di Pasquale, S. Preiss, F. Tavares Da Silva, N. Garcon, Vaccines (Basel) 2015, 3, 320.

[2]   R. Kwok, Nature 2011, 473, 436.

[3]   T. Thanh Le, Z. Andreadakis, A. Kumar, R. Gomez Roman, S. Tollefsen, M. Saville, S. Mayhew, Nat Rev Drug Discov 2020; A. Ukidve, Z. Zhao, A. Fehnel, V. Krishnan, D. C. Pan, Y. Gao, A. Mandal, V. Muzykantov, S. Mitragotri, Proc Natl Acad Sci U S A 2020.

[4]   W. S. Bowen, A. K. Svrivastava, L. Batra, H. Barsoumian, H. Shirwan, Expert Rev Vaccines 2018, 17, 207; N. Petrovsky, Drug Saf 2015, 38, 1059.

[5]   C. Agatemor, K. N. Ibsen, E. E. L. Tanner, S. Mitragotri, Bioeng Transl Med 2018, 3, 7.

[6]   E. E. L. Tanner, A. M. Curreri, J. P. R. Balkaran, N. C. Selig-Wober, A. B. Yang, C. Kendig, M. P. Fluhr, N. Kim, S. Mitragotri, Adv Mater 2019, 31, e1901103; M. Zakrewsky, K. S. Lovejoy, T. L. Kern, T. E. Miller, V. Le, A. Nagy, A. M. Goumas, R. S. Iyer, R. E. Del Sesto, A. T. Koppisch, D. T. Fox, S. Mitragotri, Proc Natl Acad Sci U S A 2014, 111, 13313.

[7]   G. D. Garcia Nores, C. L. Ly, D. A. Cuzzone, R. P. Kataru, G. E. Hespe, J. S. Torrisi, J. J. Huang, J. C. Gardenier, I. L. Savetsky, M. D. Nitti, J. Z. Yu, S. Rehal, B. J. Mehrara, Nat Commun 2018, 9, 1970; Z. Zhao, A. Ukidve, A. Dasgupta, S. Mitragotri, Adv Drug Deliv Rev 2018, 127, 3.

[8]   B. Spellberg, J. E. Edwards, Jr., Clin Infect Dis 2001, 32, 76.

[9]   H. HogenEsch, D. T. O'Hagan, C. B. Fox, NPJ Vaccines 2018, 3, 51; T. J. Moyer, Y. Kato, W. Abraham, J. Y. H. Chang, D. W. Kulp, N. Watson, H. L. Turner, S. Menis, R. K. Abbott, J. N. Bhiman, M. B. Melo, H. A. Simon, S. Herrera-De la Mata, S. Liang, G. Seumois, Y. Agarwal, N. Li, D. R. Burton, A. B. Ward, W. R. Schief, S. Crotty, D. J. Irvine, Nat Med 2020, 26, 430.

[10]   K. Cu, R. Bansal, S. Mitragotri, D. Fernandez Rivas, Ann Biomed Eng 2019.

[11]   Z. M. Zhao, Y. Hu, T. Harmon, P. Pentel, M. Ehrich, C. M. Zhang, Biomaterials 2017, 138, 46.
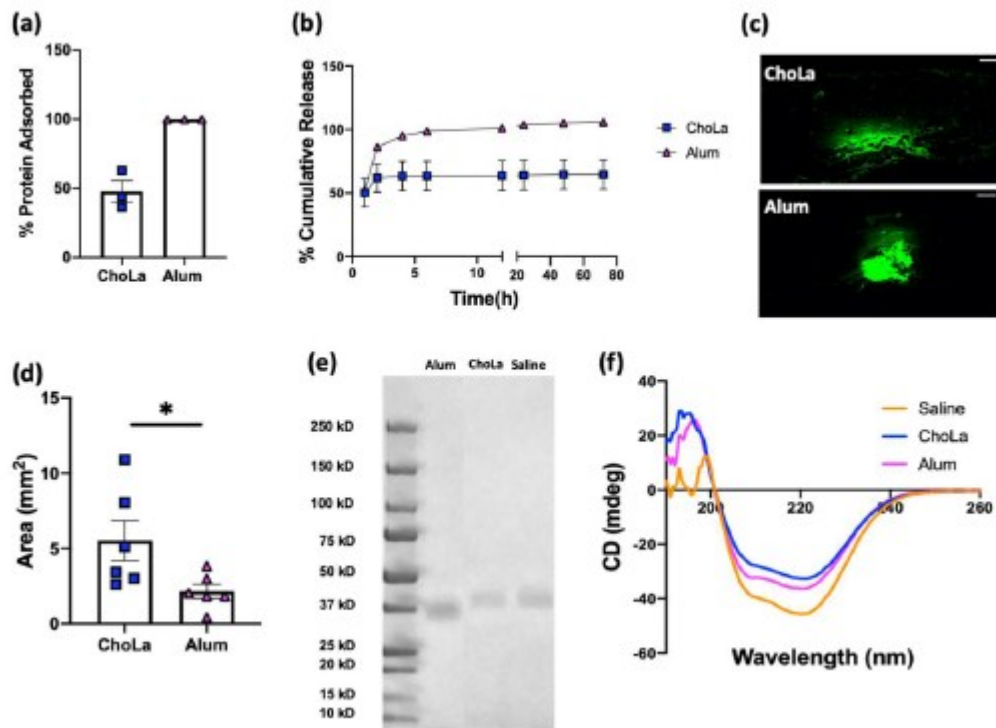
Figure 1. ChoLa adsorbs, disperses and withholds the release of OVA while maintaining integrity.
a. Percent of incubated OVA adsorbed on adjuvants (n=3 for all groups). **b.** Percent cumulative release of adsorbed OVA from two adjuvants (n=3 for all groups). **c.** Fluorescence images of porcine skin dispersion of fluorescently labeled OVA for ChoLa and alum. Scale bar: 1000 µm. **d.** Quantitative area coverage of dispersed OVA in mm^2 (n=6 for both groups). *: p<0.05. Significantly different. (Unpaired t-test) **e.** SDS-PAGE analysis of OVA with different adjuvants showing a distinct band between 37- 50 kDa, indicating stable OVA. **f.** Circular dichroism spectra demonstrating conserved α helices for all adjuvants. Data in **a**,**b**,**d** are represented as mean ± s.e.m.
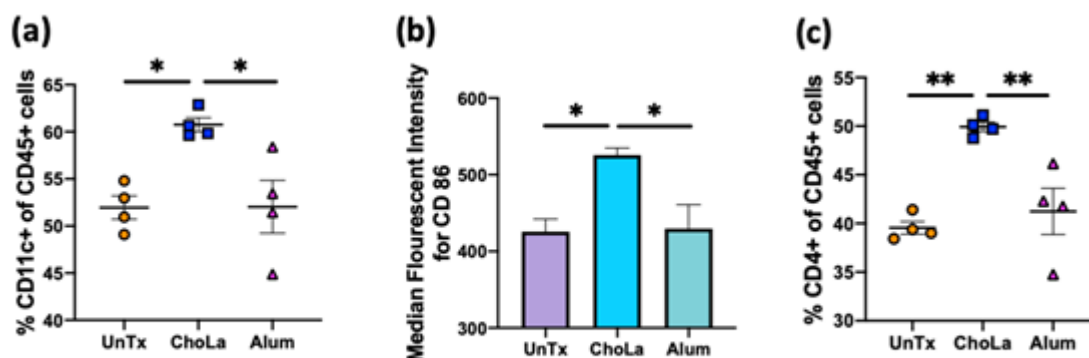
Figure 2. ChoLa improves immune infiltration at the injection site. a. Quantitative analysis of infiltrating CD11c+ of CD45+ cells (n=4 for all groups) at the injection site. **b.** Quantitative analysis of median fluorescent intensity of CD 86 on CD11c+ cells at the injection site (n=4 for all groups). **c.** Quantitative analysis of infiltrating CD4+ of CD45+ cells at the injection site (n=4 for all groups) For **a-c,** UnTx indicates untreated mice. For **a-c,** Significantly different. *: $p < 0.05$, **: $p < 0.01$ (One-way ANOVA followed by Tukey's HSD). Data in **a-c** are represented as mean ± s.e.m.
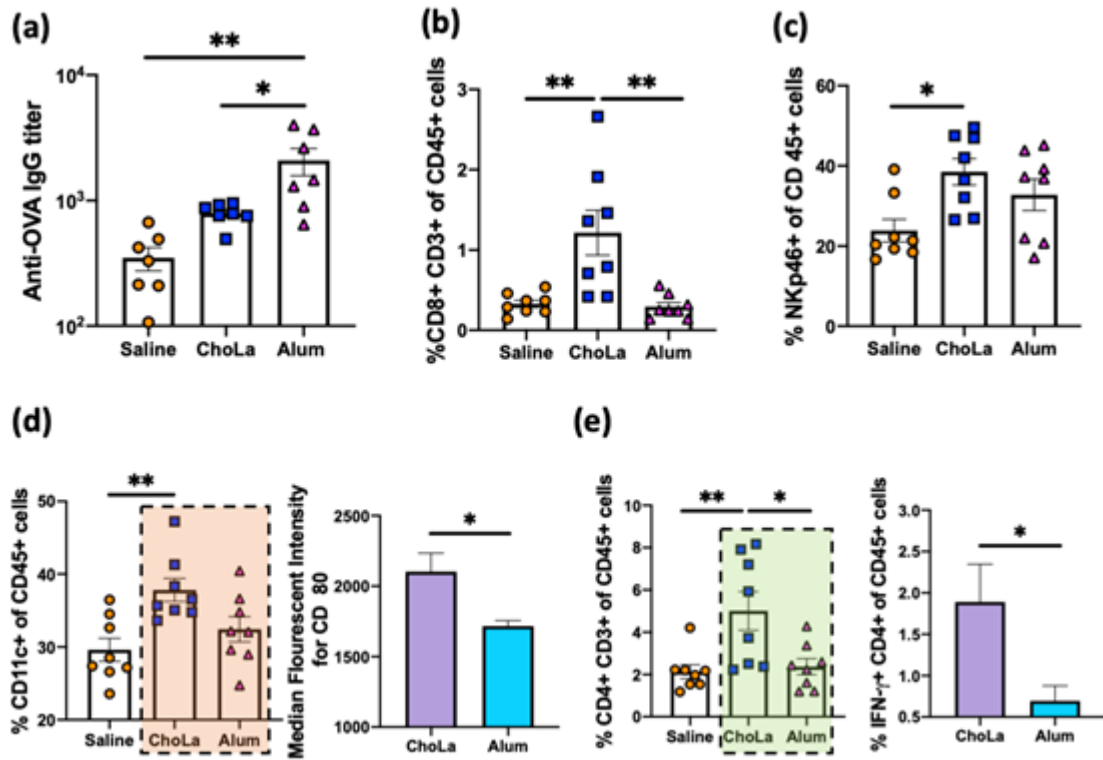
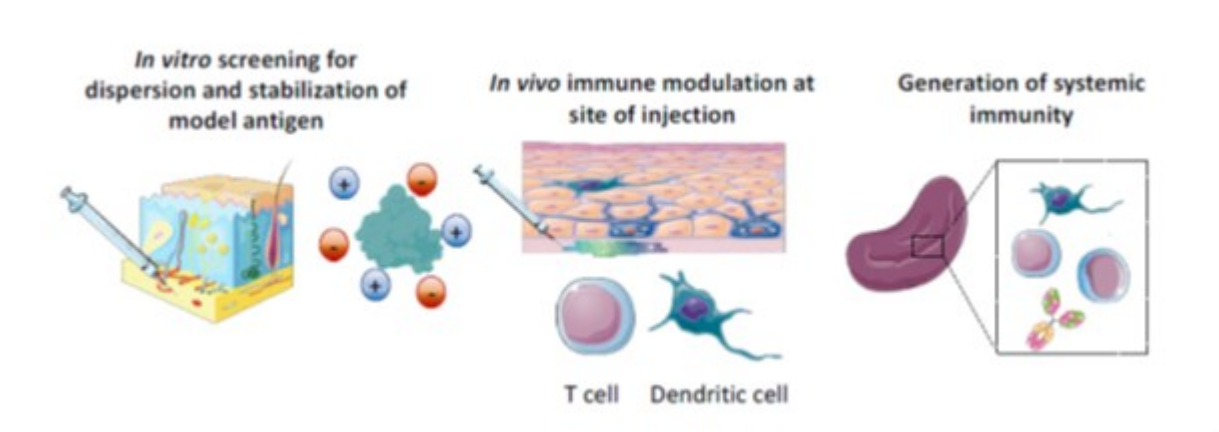**Figure 3. ChoLa vaccination leads to a potent systemic *Th1* immune responses. a.** Anti-OVA IgG antibody titer for different adjuvants (n=7 for all groups). **b.** Quantitative analysis of CD8+CD3+ of CD45+ cells (n=8 for all groups) in spleen. **c.** Quantitative analysis of NKp46+ of CD45+ cells (n=8 for all groups) in spleen. **d.** Quantitative analysis of CD11c+ of CD45+ cells (n=8 for all groups) in spleen. Orange rectangle indicates further analysis of median fluorescent intensity of CD80 for ChoLa and Alum. **e.** Quantitative analysis of CD4+CD3+ of CD45+ cells (n=8 for all groups) in spleen. Green rectangle indicates further analysis of IFN- γ+ CD4+ cells for ChoLa and Alum. For **a-e,** Significantly different. *: $p<0.05$, **: $p<0.01$ (One-way ANOVA followed by Tukey's HSD). For orange and green rectangles in **d** and **e**, significantly different. *: $p<0.05$ (Unpaired t-test). Data in **a-e** are represented as mean ± s.e.m.

Table of Contents

Despite extensive research, only a handful of vaccine adjuvants, non-native to the human body, have been approved. A new adjuvant based on ionic liquids is demonstrated, which combines two metabolites of the body, choline and lactic acid (ChoLa). It successfully enhances immune infiltration at the injection site and leads to a potent immune response against the antigen, serving as a safe adjuvant alternative that can help protect infections.

Figure:

Keyword: Novel adjuvant